JOURNAL OF CATALYSIS 81, 311–327 (1983)

Catalytic Properties of Defective Brannerite-Type Vanadates

II. A Model of Sites Active in Oxidation of Propylene on the (201) and (20$\bar{2}$) Planes of $Mn_{1-x}\phi_xV_{2-2x}Mo_{2x}O_6$

JACEK ZIÓŁKOWSKI

Institute of Catalysis and Surface Chemistry, Polish Academy of Sciences, ul. Niezapominajek, 30-239 Kraków, Poland

Received May 8, 1981; revised October 18, 1982

A model of sites active in oxidation of propylene on (201) and (20$\bar{2}$) planes of $Mn_{1-x}\phi_xV_{2-2x}Mo_{2x}O_6$ catalyst has been developed. Propylene is considered to be adsorbed on the coordinatively unsaturated surface metal atoms as a π-complex. The mechanism of its transformation is thought to depend on the number and configuration of active oxygen atoms around the adsorption center. Structural considerations are based on crystallographic data and the individual activities of surface oxygen atoms are assumed to be proportional to the reciprocal sum of the strength of bonds to them from the adjacent cations. The latter are calculated according to the bond-length–bond-strength concept. The conclusions from the model are very consistent with the experimental facts, published previously (Ziółkowski and Janas, *J. Catal.* **81,** 298 1983), which reveal important differences between the mechanism of propylene oxidation on the (201) and (20$\bar{2}$) crystallographic planes. The method applied to determine the structure of the active sites seems to have more general significance and may be applied to other oxide catalysts.

INTRODUCTION

We have recently published the results of studies on the oxidation of propylene over $Mn_{1-x}\phi_xV_{2-2x}Mo_{2x}O_6$ solid solutions (denoted by MV-X, where X = 100x) with the brannerite-type structure (*1*), where ϕ represents a vacancy at a Mn^{2+} site. Some details concerning the properties of these solids will be recalled and referred to in later paragraphs of this paper. Here we need menion only that it has been found that the morphology of the grains of MV-X catalysts depends on the conditions of their preparation and that (201) or (20$\bar{2}$) crystallographic planes may prevail in their external surfaces. A morphological factor f, defined as the ratio of the X-ray reflection intensities from the two planes ($f = I_{201}/I_{20\bar{2}}$), was taken as a semi-quantitative measure of the contribution of the planes in the grain surface. On this basis two series of MV-X preparations were selected: a so-called (201) series of high f and high contribution of the (201) plane, and a (20$\bar{2}$) series of low f and high contribution of the (20$\bar{2}$) plane. X varied along both series. When these preparations were submitted to catalytic testing a reactive specificity of the (201) and (20$\bar{2}$) crystalline faces of MV-X was observed. The reaction schemes proposed for the two faces are recalled in Fig. 1. On the (201) plane there predominate active centers capable of successive, one-by-one, incorporation of oxygen atoms into the organic molecule, separated by desorption–adsorption processes. In contrast, the active complexes formed on the K_2 and K_3 active centers of the (20$\bar{2}$) plane may decompose alternatively to the more or less oxidized products. This means that the latter centers are able to incorporate in "one stage" (i.e., without desorption) more than one oxygen atom to the molecule of propylene or to the products of its degradation. The (201) plane is much less active than (20$\bar{2}$). The common feature of both planes is that the total combustion markedly dimin-

0021-9517/83 $3.00

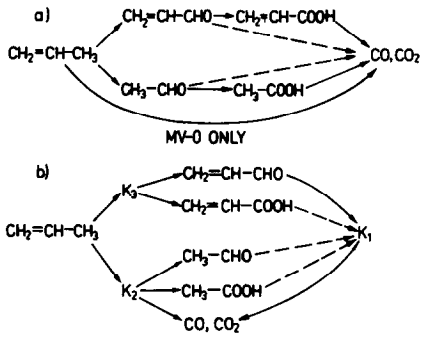

FIG. 1. Propylene oxidation schemes on the (201) (a) and (20$\bar{2}$) (b) crystallographic planes of $Mn_{1-x}\phi_xV_{2-2x}Mo_{2x}O_6$ solid solutions. Full lines represent the identified reactions, dotted lines represent the presumed reactions.

ishes with the increase of the composition parameter x. At the same time the yields of C_2 and C_3 products increase.

The abovementioned properties of the MV-X solid solutions must result from the differences in the geometry of the (20$\bar{2}$) and (201) planes and in the energetics of the surface oxygen atoms.

The aim of the present paper is the analysis of these factors. The structural considerations are based on the crystallographic data and the "activity" of surface oxygen is discussed on the basis of the bond strength (= bond valence) concept and bond-length–bond-strength dependences. The literature data concerning adsorption of propylene are also taken into account.

ADSORPTION AND TRANSFORMATIONS OF PROPYLENE ON THE SURFACE OF OXIDE CATALYSTS

The adsorption of propylene on the surface of oxide catalysts is usually considered to be the result of interactions between the molecule of propylene and coordinatively unsaturated metal cations. These interactions have been the subject of numerous works (*2–4*), the most detailed being the recent quantum-chemical computations by Haber *et al.* (*5–7*). Propylene–transition metal bonding (Fig. 2a) is assumed to be composed of (1) a σ molecular orbital formed from the highest filled π-orbital of propylene and the acceptor d_{z^2} orbital of the metal atom (the z axis is chosen to be perpendicular to the surface), and (2) a π molecular orbital resulting from the donation of electrons from the d_{xz} or d_{yz} orbitals of the metal into the lowest π^* antibonding orbital of the propylene. Adsorbed propylene is situated in the plane parallel to the surface and its orientation depends on the orientation of the d_{xz} and d_{yz} orbitals and thus on the symmetry of the local crystal field.

The reactive chemisorption of propylene on a surface metal atom results in the abstraction of an α-hydrogen atom and formation of the symmetrical chemisorbed allylic species (*3–11*). A positive charge appears at its carbon atoms (preferentially at the lateral ones) due to the shift of electrons directed to the adsorbing metal or to the bulk of a catalyst (*5–7*). This makes possible the nucleophilic attack of lattice oxygen (regarded roughly as O^{2-}) on the allyl species with formation of a new intermediate which may decompose further to acrolein.

The process of oxygen incorporation has so far been considered taking into account such parameters as oxygen bond energy (measured by catalyst reduction rate (*12*), isotopic exchange (*13–15*), or heat of oxide formation (*16, 17*)) and bond nucleophilicity (*18*). These data, however, do not permit one to distinguish between the various types of lattice oxygen which exist in complex oxide systems. Only a few attempts have been made to correlate catalytic activity in hydrocarbon oxidation with the presence of particular types of metal–oxygen bonding, e.g., Mo=O (*4, 19–23*). Practically no data have been presented so far on the effect of the number and configuration of active oxygen atoms surrounding the adsorbed molecule of propylene. One can anticipate that if these oxygen atoms are isolated, the dual site mechanism may be effectuated (*4, 7*), resulting in the addition of only one oxygen atom on one center, with selective formation of acroleine (and acrylic acid, if adsorption reiterates). On

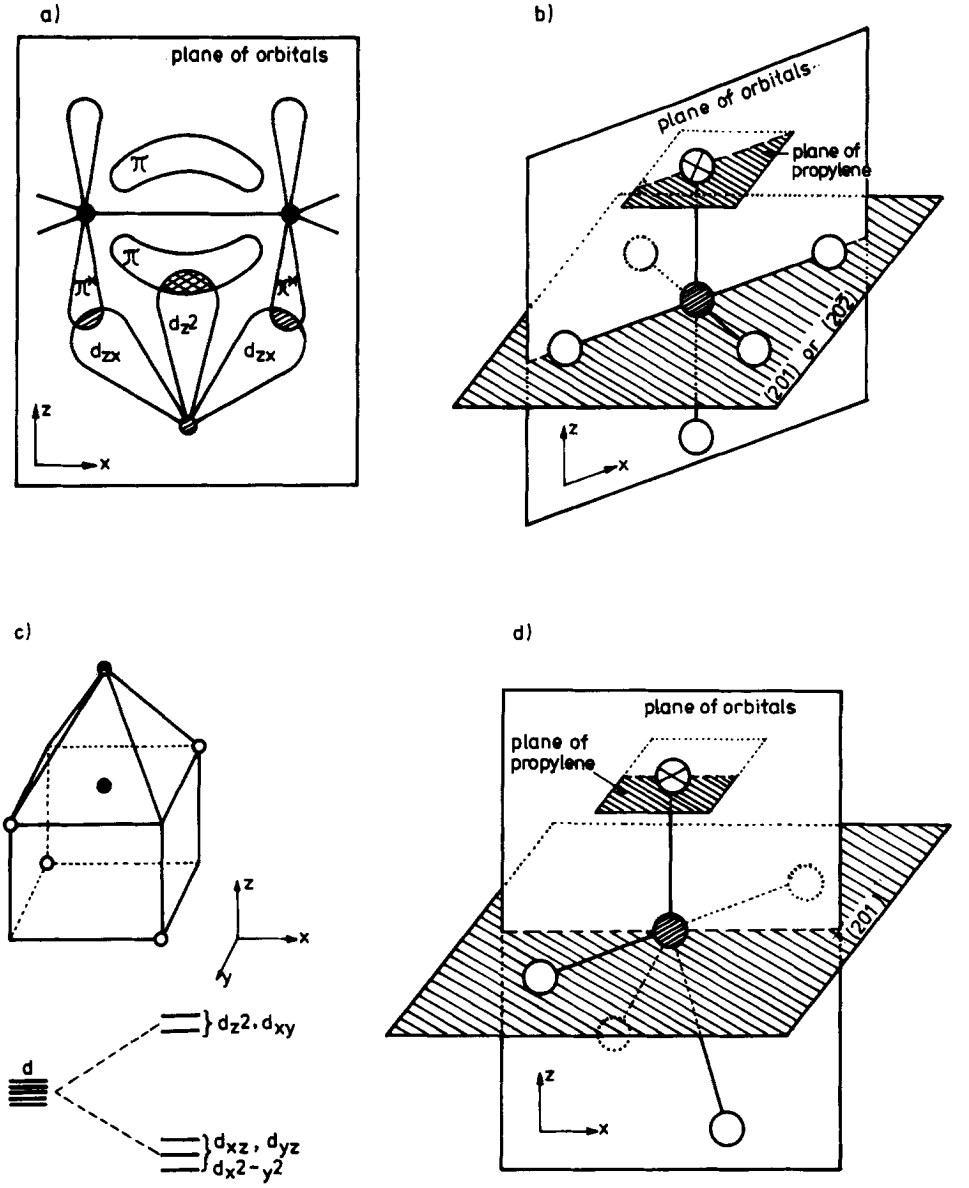

FIG. 2. Expected metal–olefin bonding and its orientation with respect to the (20$\bar{2}$) and (201) planes of MV-X. Black circles, carbon; open circles, oxygen; dashed circles, metal; crossed circle, propylene. The origin is placed on the metal atom. Planes cross one another as shown by the dotted lines. (a) Plane in which $\sigma(\pi + d_{z^2})$ and $\pi(\pi^* + d_{xz})$ molecular orbitals are formed between olefin and surface metal atom. (b) Configuration: lattice plane–plane of orbitals–plane of propylene (constituted by three carbon atoms) for the octahedral complex, valid for Mn^{2+} on the (20$\bar{2}$) plane and for V^{5+}/Mo^{6+} on both (201) and (20$\bar{2}$) planes. As explained in the text, in the latter case the weak π molecular orbital may be broken and the plane of orbitals with the plane of propylene may rotate simultaneously around the z axis. (c) Coordination of Mn^{2+} on the (201) plane and the expected splitting of d-orbitals. (d) Configuration: lattice plane–plane of orbitals–plane or propylene, valid for Mn^{2+} on the (201) plane of MV-X. All structures are idealized. In reality the polyhedra are distorted and the discussed planes are more or less inclined.

the other hand, if there are two or more active oxygens around the adsorption center and if they are conveniently arranged their simultaneous attack on different carbon atoms of propylene seems to be possible, resulting in the formation of $C_2 + C_1$ products or even in total degradation of the molecule to CO and CO_2. Similarly, attack of two active oxygens on the same lateral carbon of the adsorbed propylene may result in the direct formation of acrylic acid on one site.

The destiny of hydrogen atoms indispensably abstracted during oxidation is rarely discussed in detail in the literature. It is usually assumed that surface –OH groups are formed as intermediates. It seems evident, however, that they may combine to form water, but only on condition that the movement of hydrogen along the surface is easy. Thus it may be concluded that the abstracted hydrogen atoms do not necessarily engage the oxygen atoms localized just in the vicinity of the adsorbed propylene but that after movement they may combine with any other, distant, loosely bound oxygen to form the molecules of water. It may be assumed, moreover, that C_1 intermediates (e.g., H—C=O), once formed, may decompose to CO or may react further with the nearest adsorbed oxygen atoms to form CO_2. This model would explain the possibility of total combustion of propylene on one center, which has in fact been observed experimentally (*1*). The direct attack of the adsorbed oxygen on the molecule of propylene (resulting, as is frequently pointed out, in degradation and combustion) should not be excluded, but this is difficult to discuss due to the lack of precise data. The adsorbed oxygen atoms are thought also to take part in the subsequent combustion of preformed C_2 and C_3 products.

The above-sketched reaction model will be developed in later sections of this paper. The initial state of adsorption of propylene will be regarded as shown in Figs. 6–11. As concerns the orientation of adsorbed propylene (see the next section and Fig. 2) it will be taken into account that (1) Mn^{2+} ions are octahedrally coordinated on the $(20\bar{2})$ plane of MV-X, (2) the coordination of Mn^{2+} on the (201) plane is close to tetrahedral and that after adsorption of propylene it is completed to a fivefold one, as shown in Fig. 2c, and (3) the coordination of V^{5+} and Mo^{6+} is octahedral on both planes. As the d-shells of the last two ions are empty, back-donation plays only a minor role in π-bonding and thus a rotation of adsorbed propylene around the σ molecular orbital seems possible to attain firmer interaction with the adjacent oxygens (see Fig. 10). The slight shift of the molecule which is expected after formation of the symmetrical allylic species will be neglected. The carbon atoms will be labeled as C_α, C_β, and C_γ for convenience only, in spite of the fact that once the allyl species is formed, C_α and C_γ are not distinguishable.

THE STRUCTURE OF THE (201) and $(20\bar{2})$ PLANES OF $Mn_{1-x}\phi_xV_{2-2x}Mo_{2x}O_6$

The brannerite ($ThTi_2O_6$)-type structure, which can be generally formulated as AB_2O_6, is monoclinic with the space group *C2/m* (*24, 25*). Table 1 summarizes the structural data for some brannerite-type vanadates and Fig. 3 shows the projection of the MgV_2O_6 structure on the (010) plane. As follows from Table 1 and Fig. 3, both A and B cations are octahedrally coordinated by six oxygen atoms. BO_6 octahedra, sharing three edges, form the infinite anionic sheets parallel to the (001) plane. A atoms, binding these sheets together, are located in AO_6 octahedra, joined by two opposite edges and forming the infinite chains along the *b* axis. Both AO_6 and BO_6 octahedra are distorted. There are three different oxygen atoms in the structure: O_1(B,A,A) (1a,1,1), O_2(B,B,A) (2a,2c,2), and O_3(B,B,B) (3g,3g,3a). The notation used in parentheses to indicate the manner of threefold coordination of oxygen and the respective bond length is self-evident if compared with Table 1.

TABLE 1

Structural Data for Some Brannerite-Type AB_2O_6 Vanadates[a]

	MgV_2O_6(25)	α-CuV_2O_6(26)	β-CdV_2O_6(27)	$NaVMoO_6$(28)	MnV_2O_6(29)	MV-40(29)
a	9.279(9)	9.168(5)	9.359	9.424	9.315(3)	9.378(3)
b	3.502(2)	3.543(3)	3.568	3.656	3.536(1)	3.613(1)
c	6.731(6)	6.478(7)	6.980	7.222	6.754(2)	6.751(2)
α	—	92.25(8)	—	—	—	—
β	111.77(6)	110.34(7)	112	110.0	112.66(2)	112.18(2)
γ	—	91.88(6)	—	—	—	—
4 × A–O(1)	2.199	2.438 2.049	2.32	2.44	2.30[b]	
2 × A–O(2)	2.024	1.904	2.22	2.29	2.12[b]	
$r_{A^{2+}} + r_{O^{2-}}$(30)	2.08	2.09	2.31	2.38	2.18	
B–O(1a)	1.674	1.655	1.68	1.63	1.67[c]	1.73[d]
B–O(2a)	1.666	1.697	1.69	1.73	1.67[c]	1.73[d]
2 × B–O(3g)	1.853	1.871 1.845	1.87	1.92	1.85[c]	1.91[d]
B–O(3a)	2.111	2.056	2.09	2.15	2.11[c]	2.17[d]
B–O(2c)	2.671	2.588	2.46	2.47	2.67[c]	2.73[d]

[a] Distances in Å, angles in degrees.
[b–d] Assumed values of Mn-O, V-O, and Mo-O distances in MV-X, respectively, as explained in the text.

There is sufficient experimental proof that MnV_2O_6 crystallizes in the brannerite-type structure with parameters very close to those of MgV_2O_6 (*29*); however, the atomic positions have never been exactly determined. On doping with MoO_3 the structure type is preserved but the lattice parameters change slightly. It is evident that in the case of solid solutions the dimensions of the BO_6 octahedra and thus the respective atomic positions should be locally different in the lattice, depending on the

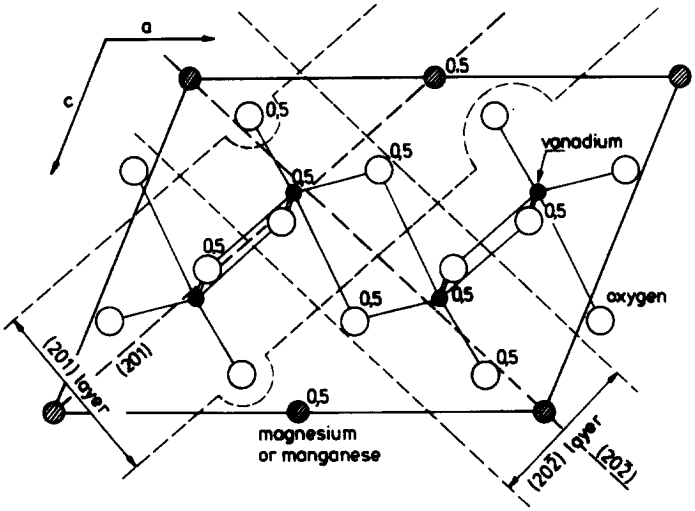

FIG. 3. Projection of the MgV_2O_6 (~MnV_2O_6) structure on the (010) plane. Marked atoms lie at y = 0.5, the others at y = 0.

kind of B atom. The same is valid for AO_6 octahedra which may be filled (Mn) or empty (ϕ).

From Table 1 it follows that (1) the differences between the lattice parameters for MnV_2O_6 and MgV_2O_6 are less than 1%, (2) the average A–O distances in AO_6 octahedra of different vanadates increase proportionally with the sum of the ionic radii of the cation and oxygen, (3) V–O distances in VO_6 groups are slightly influenced by the kind of A atom,[1] and (4) the main effect of substitution of the larger Mo^{6+} for the smaller V^{5+}, as with $NaVMoO_6$, is the increase of most B–O distances.[1]

Bearing in mind the above observations it was decided to construct the (201) and (20$\bar{2}$) planes of MnV_2O_6 based on the structural data for MgV_2O_6. On the other hand, for the purpose of the quantitative bond strength calculations (see the next section) the distances A–O and B–O taken from the MgV_2O_6 structure were enlarged by differences of the respective ionic radii ($r_{Mn^{2+}} - r_{Mg^{2+}} = 0.10$ Å, $r_{Mo^{6+}} - r_{V^{5+}} = 0.06$ Å) (*30*). The respective assumed bond length values are indicated in Table 1.

As already mentioned, the projection of the MgV_2O_6 (~MnV_2O_6) structure on the (010) plane is presented in Fig. 3. Both planes under discussion, viz. (201) and (20$\bar{2}$), are perpendicular to (010) and intersect it as marked in Fig. 3. Due to the relatively low symmetry of the lattice, only a few atoms lie exactly in the above-indicated two-dimensional planes. Thus, representative layers are examined, chosen in such a manner as to cut the weakest bonds and to have the chemical composition MnV_2O_6 for the layer. It is evident that the whole crystal may be constructed by stacking up such layers. The arrangement of the (201) and (20$\bar{2}$) surface layers is visualized in Fig. 4. The oxygen atoms differing in bond type coordination are labeled by different capital letters. The oxygen atoms lying above the surface layers and completing the polyhedra around A and B are regarded as adsorbed atoms and are drawn with dotted circles.

[1] Except for the longest V–O or Mo–O bond, which is, however, of minor importance in Σs_i calculations (cf. the next paragraph).

BOND STRENGTH CONCEPT

The concept of the electrostatic bond strength (s) was defined by Pauling (*31*) as the valence (z_c) of a cation divided by its coordination (ν). He stated that in a stable ionic structure the valence of each anion (z_a) is exactly or nearly equal to the sum of the strength of the bonds to it from the adjacent cations ($z_a \approx \Sigma s_i = \Sigma z_c/\nu$). Deviations from this rule were usually interpreted by stating that the bond strength must depend on anion–cation distances (R). Different analytical expressions (see, e.g., Eq. (1)) for the s–R dependence have been proposed and reviewed, e.g., in Refs. (*32–34*). The best analytically determined data for s now fit Pauling's rule with an accuracy of several percent and they are even used at present as an additional test of the correctness of structure resolution. It has moreover been pointed out (*34*) that the concept of bond strength can also be used in the situation where the binding is primarily covalent and thus terms like "cation" or "anion" are used for convenience only.

The author's idea was to take the Σs_i values of the surface oxygen atoms as the measure of their binding energy, and consequently as the measure of their "activity" in catalytic reactions, activity being proportional to the reciprocal of Σs_i. A simplified assumption is that the positions of the surface oxygens are the same as those in the bulk of the lattice.

The present calculations are based on the most recent data by Brown and Wu (*35*) who proposed the following empirical relation between the bond strength s and bond length R:

$$s = (R/R_1)^{-N} \qquad (1)$$

where R_1 is the length expected for a bond of unit valence and N gives the slope of the

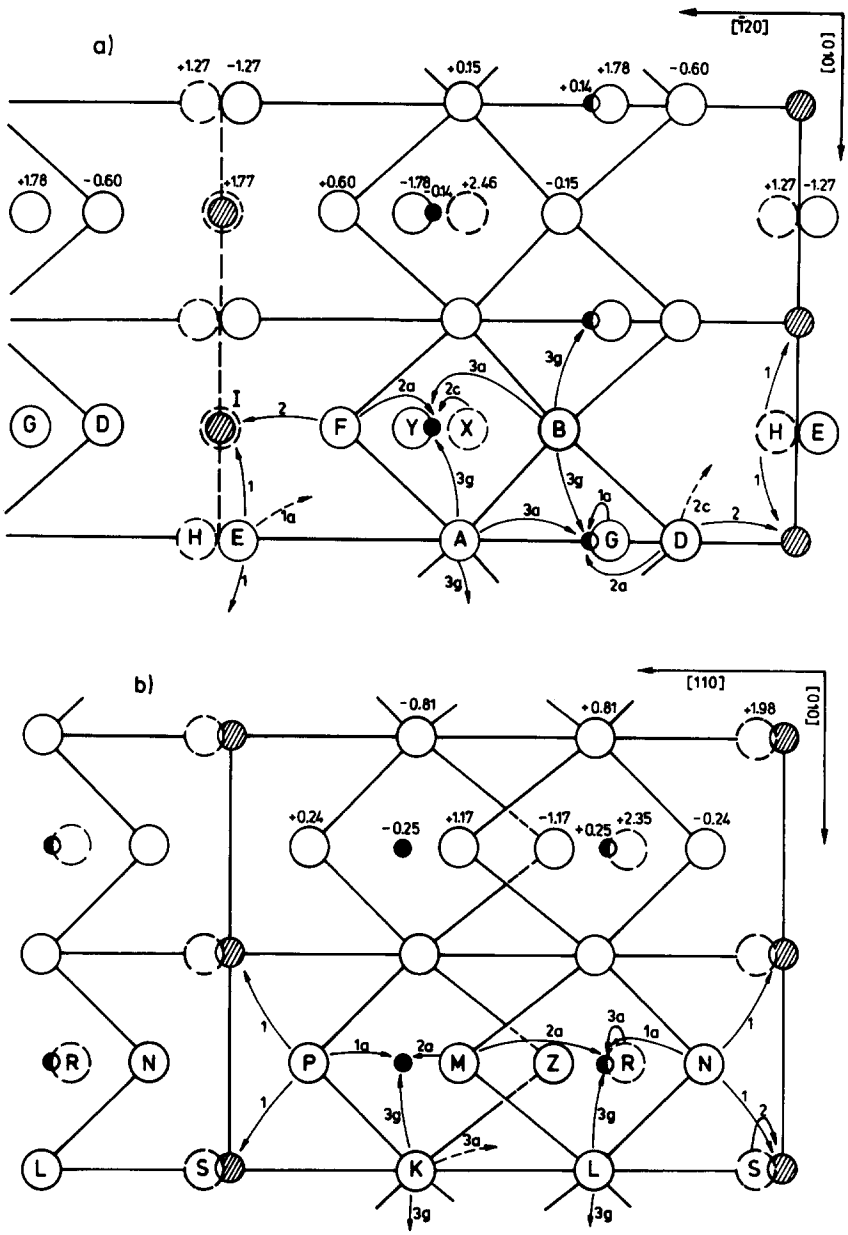

FIG. 4. The arrangement of (a) (201) and (b) $20\bar{2}$) surface layers of MnV_2O_6. Mn, V, and O atoms are marked as in Fig. 3. Mn atoms lie exactly in the respective planes, the distances (in Å) of the other atoms localized up and down the planes are indicated in the figure. Oxygen atoms of different bonding (1, 2, 1a, 2a, etc.) are labeled with different capital letters A–Z (cf. Tables 1, 2, and 3). Bonds marked with dotted lines are directed to the bulk. Dotted circles represent the adsorbed oxygen atoms.

$s = f(R)$ curve. The empirical constants R_1 and N have been determined in the quoted work for 84 different cations in an oxygen environment, using the experimental data for environments of 936 cations in various crystal structures and the statistical procedure described in Ref. (*34*). In particular $s_{Mn^{2+}-O} = (R/1.798)^{-5.6}$, $s_{V^{5+}-O} = (R/1.791)^{-5.1}$, and $s_{Mo^{6+}-O} = (R/1.882)^{-6}$. Using these expressions and the interatomic dis-

TABLE 2

Bond Strength of Oxygen Atoms on the (201) Plane

Type of oxygen	Bonding	Cation coordination	Σs_i	Population composition dependence (cf. Fig. 5)
$O_A = O_B$	(3g, 3g, 3a)	(V, V, V)	2.11	$(1-x)^3$ III′
		(V, V, Mo)	2.10	$x(1-x)^2$ IV
		(V, Mo, V)	2.18	$2x(1-x)^2$ V
		(V, Mo, Mo)	2.17	$2x^2(1-x)$ V′
		(Mo, Mo, V)	2.24	$x^2(1-x)$ IV′
		(Mo, Mo, Mo)	2.24	x^3 III
O_D	(2a, 2c, 2)	(V, V, Mn)	1.97	$(1-x)^3$ III′
		(V, V, ϕ)	1.58	$x(1-x)^2$ IV
		(V, Mo, Mn)	1.95	$x(1-x)^2$ IV
		(V, Mo, ϕ)	1.55	$x^2(1-x)$ IV′
		(Mo, V, Mn)	2.20	$x(1-x)^2$ IV
		(Mo, V, ϕ)	1.81	$x^2(1-x)$ IV′
		(Mo, Mo, Mn)	2.18	$x^2(1-x)$ IV′
		(Mo, Mo, ϕ)	1.79	x^3 III
O_E	(1a, 1, 1)	(V, Mn, Mn)	1.93	$(1-x)^3$ III′
		(V, Mn, ϕ)	1.68	$2x(1-x)^2$ V
		(V, ϕ, ϕ)	1.42	$x^2(1-x)$ IV′
		(Mo, Mn, Mn)	2.15	$x(1-x)^2$ IV
		(Mo, Mn, ϕ)	1.90	$2x^2(1-x)$ V′
		(Mo, ϕ, ϕ)	1.65	x^3 III
O_F	(—, 2a, 2)	(—, V, Mn)	1.84	$(1-x)^2$ II′
		(—, V, ϕ)	1.45	$x(1-x)$ VI
		(—, Mo, Mn)	2.07	$x(1-x)$ VI
		(—, Mo, ϕ)	1.68	x^2 II
O_G	(1a, —, —)	(V, —, —)	1.42	$(1-x)$ I′
		(Mo, —, —)	1.65	x I
O_H	(—, 1, 1)	(—, Mn, Mn)	0.50	$(1-x)^2$ II′
		(—, Mn, ϕ)	—	— —
		(—, ϕ, ϕ)	—	— —
O_I	—	(Mn, —, —)	0.2	$(1-x)$ I′
		(ϕ, —, —)	—	— —
O_X	(2c, —, —)	(V, —, —)	0.13	$(1-x)$ I′
		(Mo, —, —)	0.11	x I
O_Y	(1a, 1, 1)	Considered as bulk atom		

tances for MV-X solid solutions discussed in the previous section and included in Table 1, the values of Σs_i were calculated for all O_A to O_Z surface oxygen atoms as shown in Tables 2 and 3. As can be seen, they vary widely and change with the composition parameter x. It has been found useful to assume that the lattice oxygen atoms of Σs_i = 1.85 to 2.25 are firmly bound and catalytically inactive, whereas those of Σs_i = 1.40 to 1.85 are regarded as loosely bound, active lattice oxygens. The Σs_i values for loosely bound adsorbed oxygen atoms (which are regarded also as active) are lower than 0.5. Strictly speaking, the activity of oxygen atoms should be regarded as changing continuously with Σs_i and the limit value of 1.85 has a tentative character. Positions of loosely bound oxygen are expected to be partly occupied, depending on Σs_i (the higher Σs_i, the higher the coverage). Under these assumptions the interactions between adsorbed propylene and surface oxygen atoms will be discussed in the next section of the paper. It should be recalled that propylene may be adsorbed over coordinatively unsaturated Mn and V/Mo atoms. On each of the discussed planes of MV-X there is one type of Mn atom, but two structurally different V/Mo atoms. To distinguish between them, they are indexed with the same letter as the oxygen position over the respective V/Mo. Thus we deal with V/Mo_G and V/Mo_X on the (201) plane and with V/Mo_M and V/Mo_R on the $(20\bar{2})$ plane.

On the basis of simple equations expressing the probability of independent events, the populations P of different oxygen atoms as a function of composition have also been calculated as shown in Fig. 5 and in Tables

TABLE 3

Bond Strength of Oxygen Atoms on the $(20\bar{2})$ Plane

Type of oxygen	Bonding	Cation coordination	Σs_i	Population–composition dependence (cf. Fig. 5)
O_K	(3g, 3g, 3a)	(V, V, V)	2.11	$(1-x)^3$ III′
		(V, V, Mo)	2.10	$x(1-x)^2$ IV
		(V, Mo, V)	2.18	$2x(1-x)^2$ V
		(V, Mo, Mo)	2.17	$2x^2(1-x)$ V′
		(Mo, Mo, V)	2.24	$x^2(1-x)$ IV′
		(Mo, Mo, Mo)	2.24	x^3 III
O_L	(3g, 3g, —)	(V, V, —)	1.68	$(1-x)^2$ II′
		(V, Mo, —)	1.75	$2x(1-x)$ VII
		(Mo, Mo, —)	1.81	x^2 II
O_M	(2a, 2c, —)	(V, V, —)	1.58	$(1-x)^2$ II′
		(V, Mo, —)	1.55	$x(1-x)$ VI
		(Mo, V, —)	1.81	$x(1-x)$ VI
		(Mo, Mo, —)	1.79	x^2 II
$O_N = O_P$	(1a, 1, 1)	(V, Mn, Mn)	1.93	$(1-x)^3$ III′
		(V, Mn, ϕ)	1.68	$2x(1-x)^2$ V
		(V, ϕ, ϕ)	1.42	$x^2(1-x)$ IV′
		(Mo, Mn, Mn)	2.15	$x(1-x)^2$ IV
		(Mo, Mn, ϕ)	1.90	$2x^2(1-x)$ V′
		(Mo, ϕ, ϕ)	1.65	x^3 III
O_R	(3a, —, —)	(V, —, —)	0.43	$(1-x)$ I′
		(Mo, —, —)	0.42	x I
O_S	(—, —, 2)	(—, —, Mn)	0.39	$(1-x)$ I′
		(—, —, ϕ)	—	— —
O_Z	(2a, 2c, 2)	Considered as bulk atom		

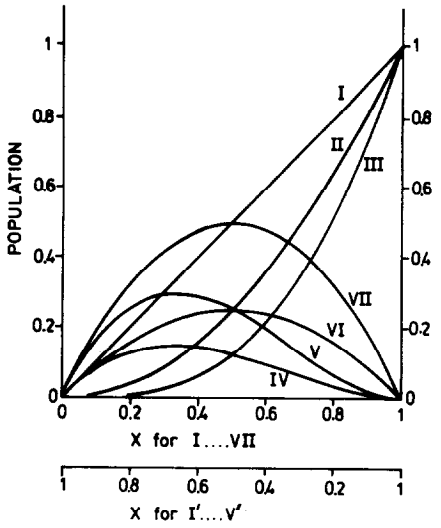

FIG. 5. Population–composition dependences (cf. Tables 2 and 3).

2 and 3. The respective P–x curves give only rough information, since an unknown chemical factor has not been taken into account. One may expect, for instance, that the configuration O_D (Mo,V,ϕ) will be preferred to O_D (Mo,V,Mn), as in the former case two defects introduced into the lattice are locally compensated. On the other hand, the population calculated for the adsorbed oxygen reflects the number of adsorption centers rather than the real coverage.

INTERACTIONS OF PROPYLENE WITH ACTIVE CENTERS ON THE (201) AND ($20\bar{2}$) PLANES OF MV-X[2]

(201) V_G and (201) Mo_G Centers (Fig. 6)

For undped MV-O there are only two active oxygen atoms in the nearest neighborhood of adsorbed propylene: these are the O_G (1.42) atom and the adsorbed O_H (0.50) or O_I (~0.2) atom (if H and I positions are occupied at all). Acrolein containing O_G (O_G–C_α–C_β–C_γ) seems thus to be the most probable reaction product with O_H or O_I eventually used to bind the abstracted hydrogens. Acrolein adsorbed again on a similar center may be transformed further to acrylic acid.

On doping, some O_G atoms become somewhat less active (1.65) and the population of O_H and O_I should diminish due to the appearance of ϕ in the original Mn sites. On the other hand, some of the O_D atoms may be activated (1.55–1.81) if the adjacent Mn position is empty. In this case epoxy-type intermediates C_α—C_β—C_γ (Fig. 6a) or

C_γ—C_β—C_α (Fig. 6b) may be formed

giving rise to C–C bond breaking. In the case of simultaneous action of, e.g., O_G on C_α and O_D on C_γ (Fig. 6b), acetaldehyde O_G–C_α–C_β and carbon monoxide C_γ–O_D are expected as reaction products.

(201) V_X and (201) Mo_X Centers (Fig. 7)

Propylene adsorbed on (201) V_X is surrounded by three active lattice oxygens, namely two O_G (1.42) and one O_F (1.84), and by adsorbed O_X (0.13). Each carbon atom of propylene may be attacked by at least one active oxygen which should cause total combustion. On doping with MoO_3, the activity of each of the above-quoted oxygens slightly changes, but the resulting action is expected to be the same.

As O_X is very weakly bonded to (201) V_X or (201) Mo_X, the same may be expected for propylene. Consequently this site should play only a minor role in the overall reaction. This conclusion is in agreement with experimental data (*1*), as the observed initial selectivity to C_1 products on (201) plane is negligible, except for MV–0.

(201) Mn Center (Fig. 8)

For MV–0 propylene adsorbed on an Mn center may interact with O_F (1.84) and O_G (1.42). Depending on the orientation, C_α and C_γ (Fig. 8a) or C_β and C_γ (Fig. 8b) may be attacked by oxygen giving rise to the formation of C_1 + C_2 products: these are

[2] For the reader's convenience the conclusions of this section are summarized in Table 4.

TABLE 4

Summary of the Structure of and Yield from Active Centers on the (201) and (20$\bar{2}$) Planes of $Mn_{1-x}\phi_xV_{2-2x}Mo_{2x}O_6$ Solid Solutions[a]

Centers	MV−0		MV−X, X > 0	
	Active oxygens	Products	Active oxygens	Products
(201) V/Mo$_G$	O_G (1.42) O_H (0.50) O_I (~0.2)	O—C—C=C	O_G (1.42 or 1.65) O_D (1.55–1.81) O_H (0.50) O_I (~0.2)	O—C—C=C O—C—C + O—C
(201) V/Mo$_X$	2 × O_G (1.42) O_F (1.84) O_X (0.13)	(O—C)[b] (O—C—O)[b]	2 × O_G (1.42 or 1.65) O_F (1.45–1.84) O_X (0.13 or 0.11)	(O—C)[b] (O—C—O)[b]
(201) Mn	O_G (1.42) O_F (1.84) O_I (~0.2)	O—C—C + O—C (O—C)	O_G (1.42 or 1.65) O_F (1.84) O_I (~0.2)	O—C—C=C O—C—C + O—C
(20$\bar{2}$) V/Mo$_M$	O_M (1.58) O_L (1.68) O_R (0.43)	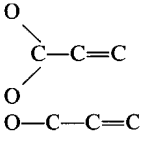	O_M (1.55–1.81) O_L (1.68–1.81) O_P (1.42–1.68) O_R (0.42 or 0.43)	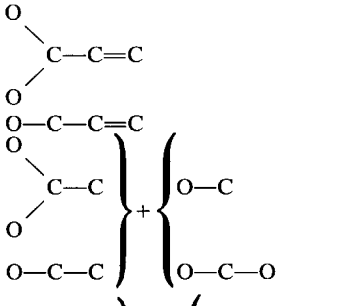
(20$\bar{2}$) V/Mo$_R$	O_M (1.58) 2 × O_L (1.68) 2 × O_S (0.39)	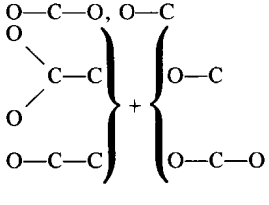	O_M (1.55–1.81) 2 × O_L (1.68–1.81) O_N (1.42–1.68) O_S (0.39)	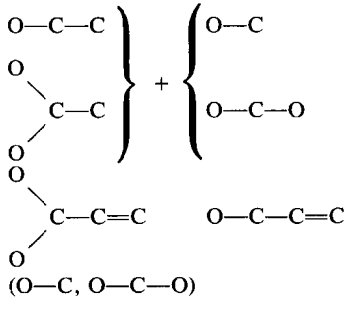

$(20\bar{2})$ Mn	O_S (0.39) (O_R (0.43))	Inactive	$2 \times O_N$ (1.68) $2 \times O_P$ (1.68) O_S (0.39) (O_R (0.43 or 0.43))	

[a] Products indicated in the table are expected to be formed at short contact time. Consecutive reactions are discussed in the text. Reaction products are ordered in decreasing probability of formation, and those placed in parentheses are presumed.
[b] Expected minor yield due to the very weak adsorption of propylene on this site.

O_G–C_α–C_β and C_γ–O_F (Fig. 8a) or C_α–C_β–O_G and C_γ–O_F (Fig. 8b), the intermediate complexes being neither of epoxy nor of peroxy-type. An action of adsorbed O_H seems to be impossible due to steric hindrance, and that of O_I seems doubtful as they are usually far from the adsorbed molecule of propylene. However, in the situation presented in Fig. 8b the total combustion of propylene (C_γ–O_F + C_β–O_G + C_α–O_I) is not to be excluded.

On doping, the participation of O_I should diminish, the activity of some of O_G slightly decrease (1.65) and some of O_F become inactive (2.07). Due to these facts the formation of C_1 and C_2 products should be quenched and acrolein O_G–C_α–C_β–C_γ should remain the most probable reaction product. It should be recalled that as we are discussing the adsorption of propylene over Mn, the Mn position must not be empty and activation of O_F to O_F (1.45) or O_F (1.68) is impossible (cf. Table 2).

Summarizing the above considerations concerning the (201) plane one may conclude that acrolein and acetaldehyde may be formed on Mn and V/Mo_G centers. An increase of the composition parameter x favors the formation of acrolein on the Mn center at the expense of acetaldehyde and the V/Mo_G center behaves conversely. Repeated interactions of acrolein and acetaldehyde with the centers of the same type may transform them consecutively to acrylic acid and acetic acid, respectively. The nature of acetaldehyde readsorption, however, is not quite clear. The subsequent combustion of preformed C_3 and C_2 products should diminish with increase of the composition parameter x due to the decrease of the concentration of adsorbed oxygen. The above conclusions are in good agreement with the experimental facts (*1*). The "one-stage" total combustion of propylene is possible on the V/Mo_X center, which plays, however, a negligible role due to the weak adsorption of propylene. This process is also possible for MV–0 on the Mn center but the probability of such a

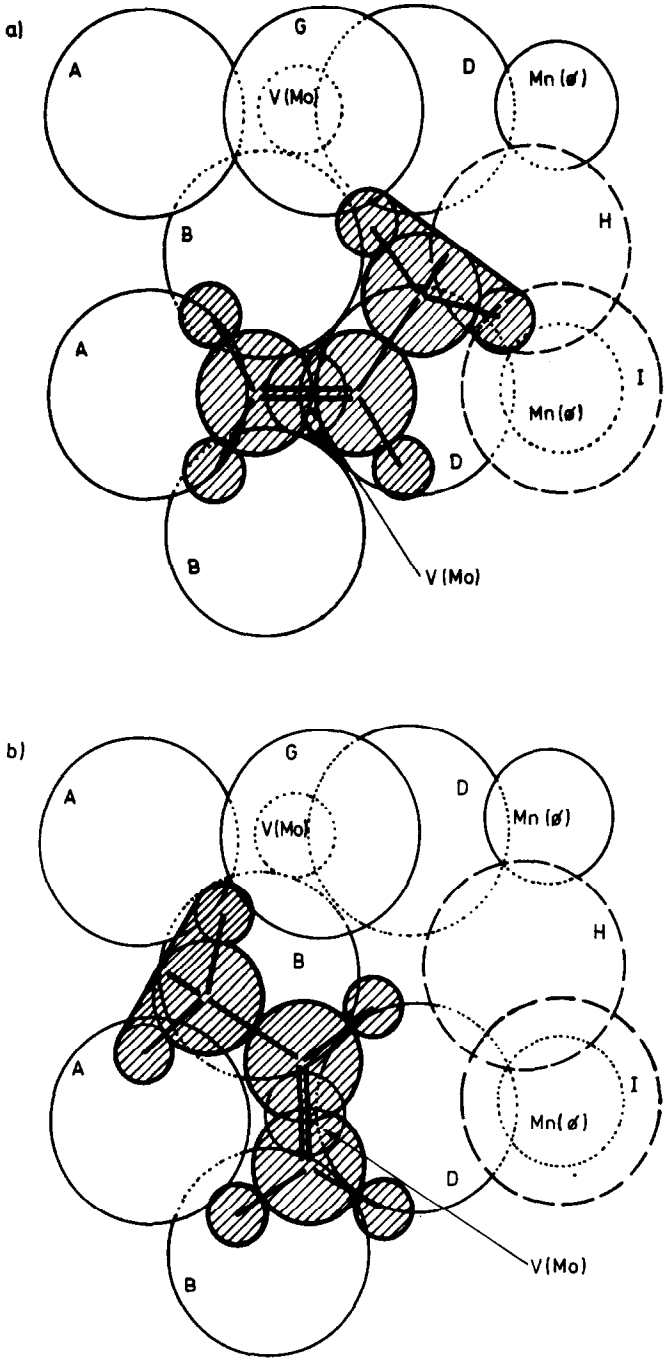

FIG. 6. Propylene adsorbed on the (201) V/Mo_G site in two configurations. Dashed circles represent the adsorbed oxygen atoms, dotted circles represent the covered atoms.

transformation is very small. As already pointed out in Ref. (*1*), the "one-stage" combustion of propylene experimentally observed for MV-0 with the (201) plane prevailing in the grain surface is due rather to the simultaneous presence of the $(20\bar{2})$ plane, which cannot be entirely eliminated in the case of three-dimensional grains.

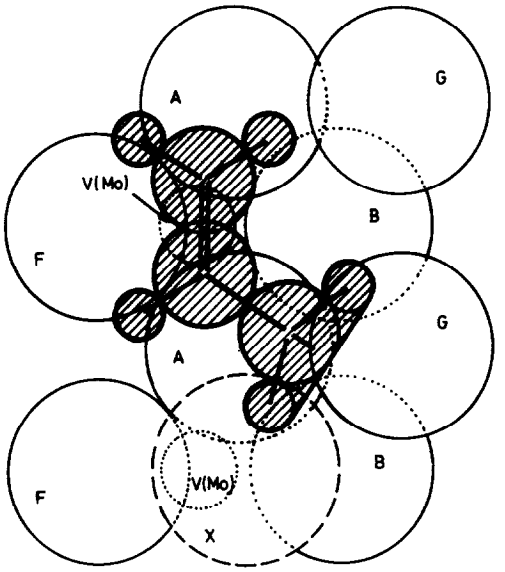

FIG. 7. Propylene adsorbed on the (201) V/Mo$_X$ site.

(20$\bar{2}$) V_M and (20$\bar{2}$) Mo_M Centers (*Fig. 9*)

There are two active lattice oxygens in the vicinity of propylene adsorbed over (20$\bar{2}$) V_M, O_M (1.58), and O_L (1.68), which may attack the same lateral C_α carbon atom. The center should thus yield, selectively, acrolein or acrylic acid. The adjacent O_R (0.43) is expected to be eventually consumed in the formation of water. On doping, the activity of O_M and O_L slightly decreases and some O_P close to C_γ are activated. Thus the center should yield $C_2 + C_1$ products besides acrolein and acrylic acid.

(20$\bar{2}$) V_R and (20$\bar{2}$) Mo_R Centers (*Fig. 10*)

A molecule of propylene adsorbed on the V_R center of the (20$\bar{2}$) plane of MV–0 is surrounded by three active lattice oxygen atoms, viz. two O_L (1.68) and one O_M (1.58), and, if adsorption centers are occupied, by two O_S (0.39). Numerous interactions and numerous intermediates can be visualized. As an example, consider the possible peroxy-type complex $C_\gamma—C_\beta—C_\alpha$ with $O_L—O_M$ (Fig. 10a) (with the possibility of simultaneous attack of the second O_L on C_α) or the

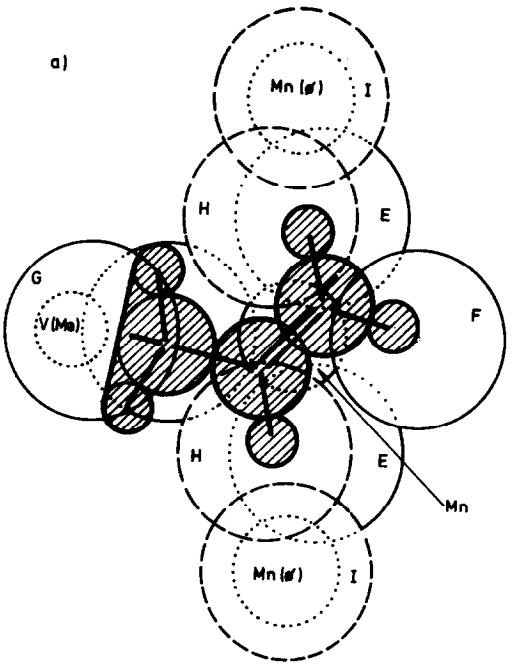

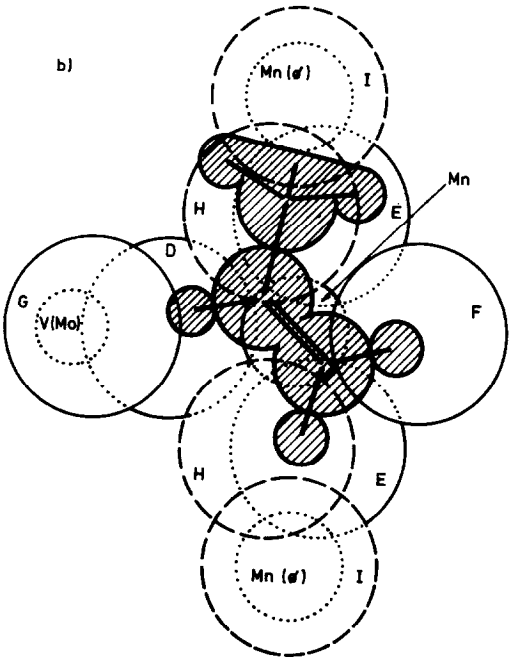

FIG. 8. Propylene adsorbed on the (201) Mn site in two configurations.

epoxy-type complex $C_\gamma—C_\beta—C_\alpha$ with O_L (Fig. 10b) (with the possibility of simultaneous attack of O_M on C_γ and the second O_L on

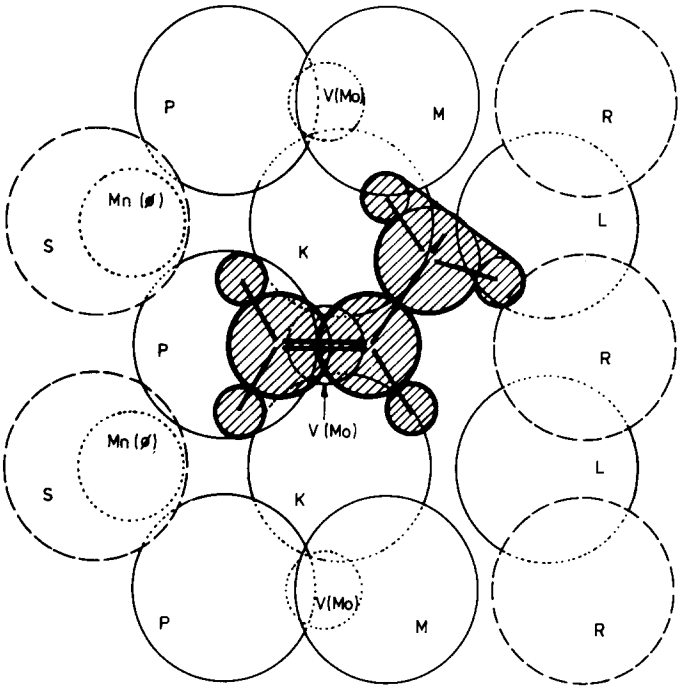

FIG. 9. Propylene adsorbed on the (20$\bar{2}$) V/Mo_M site.

C_α, C_β, or C_γ). Both of them may make the first step of molecule degradation and additional interactions indicated above in parentheses may even give rise to total combustion. Participation of O_S in the reaction is also possible. Avoiding too speculative and detailed considerations, one may generally conclude that the number of active oxygens around the discussed center is sufficient to transform propylene to more (acetic acid + C_1, "one-stage" total combustion) or less (acetaldehyde + CO) oxidized products. Formation of acrolein and acrylic acid is hardly possible on this center.

On doping, the following changes around

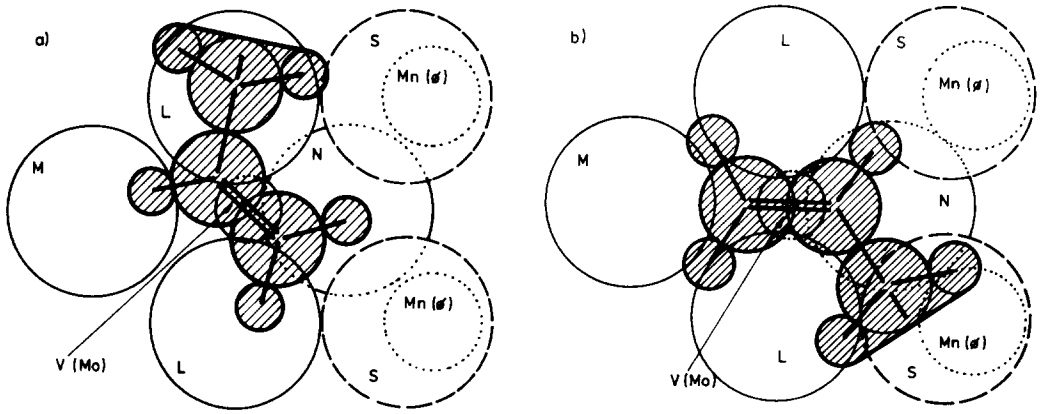

FIG. 10. Propylene adsorbed on the (20$\bar{2}$) V/Mo_R site in two configurations.

the V/Mo$_R$ center are expected: (1) decrease of the O_S concentration due to the appearance of ϕ instead of Mn, (2) decrease of activity of some of the O_L and O_M, and (3) activation of the fourth of the lattice oxygens O_N (cf. Table 3).

Of the above effects the first two should result in a decrease of total combustion, as was in fact observed experimentally. As concerns the second and the third effect it seems important to stress that the changes in activity of O_N, O_M, and two O_L are independent, as they are coordinated by different cations. The activity of O_N depends on the presence of Mn or ϕ in the original Mn site which does not affect the activity of O_M and O_L. On the other hand, O_M and O_L are each bound to two V/Mo atoms, only one of them being common. These facts increase the variety of possible interactions between the surface and adsorbed propylene, the expected tendency increasing with doping, being a preference of partial oxidation to C_2 + C_1 or to C_3 products. If, for instance, the discussed adsorption center is surrounded by two O_L (Mo,Mo,—) (1.81), O_M (Mo,Mo,—) (1.79), and O_N (Mo,ϕ,ϕ) (1.65), the last of them becomes the most active and in the configuration presented in Fig. 10a its interaction with C_γ should preferentially result in the formation of acrolein at the expense of C_2 and C_1 products.

(20$\bar{2}$) Mn Center (Fig. 11)

Propylene adsorbed on the Mn center of the (20$\bar{2}$) plane is surrounded by two lattice O_N and two lattice O_P atoms and eventually by adsorbed O_S and O_R atoms, the two latter being rather distant. The abovementioned lattice oxygens are inactive (1.93) in the MV-0 sample. On doping, some of them may be activated if coordination (V,Mn,ϕ) (1.68) is attained. As there are four of them various interactions with propylene and various intermediates (similar to those already discussed for (20$\bar{2}$) V/Mo$_R$ center) may be considered. The probability of simultaneous activation of all four O_N and O_P atoms is, however, very small. If

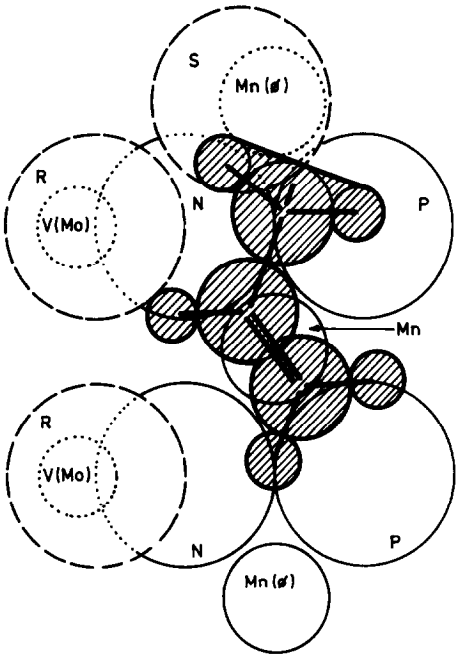

FIG. 11. Propylene adsorbed on the (20$\bar{2}$) Mn site.

one of the adjacent Mn positions is vacant, one pair (O_N, O_P) is activated which may rather attack one of the lateral carbons of propylene. It is thus to be expected that the (20$\bar{2}$) Mn center should be less active than the (20$\bar{2}$) V/Mo$_R$ center but more selective to the less oxidized products, in particular to the C_3 ones.

It follows from the above considerations that the (20$\bar{2}$) plane is much richer in active oxygen atoms than the (201) plane. It is thus understandable that the former plane is more active then the latter, as found experimentally. It has been shown, moreover, that the adsorption sites on the (20$\bar{2}$) plane are usually surrounded by several active oxygens and thus two oxygen-containing acids and other highly oxidized products may be formed in "one stage" there. The discussion above demonstrates also that on the (20$\bar{2}$) plane a decrease of selectivity to C_1 products and an increase of the ratio (selectivity to C_3)/(selectivity to C_2) is expected on passing from MV-0 to MV-10 or to MV-30, as observed experimentally (*1*).

The main conclusions of this section concerning the structure of the active centers, the most probable reaction products, and their dependence on composition and crystallographic face specificity are gathered together in Table 4.

CONCLUSIONS

A model for the active sites on the (201) and (20$\bar{2}$) planes of the brannerite-type structure has been developed. Activities of the individual surface oxygen atoms have been calculated on the assumption that they are proportional to the reciprocal sums of the strength of bonds to them from the adjacent cations. So far, the activity of surface oxygen was usually determined by experimental methods (reducibility, isotopic exchange, heat of formation) providing integral information. The determination of the individual activities has made possible a more detailed discussion of the structure and action of active sites comprising such details as the dependence of the reaction path on the configuration and the number of the nearest active oxygen atoms. It is particularly interesting that the same adsorption site may bear a number of different catalytically active centers depending on the activation or deactivation of the adjacent oxygens by structural defects in the second coordination sphere.

As shown in the previous section, the model agrees well with the experimental facts published previously (*1*) and reveals important differences between the mechanism of oxidation of propylene on the two crystallographic planes under discussion. It should be stressed that each of the active centers labeled previously as K_1, K_2, and K_3 (cf. Fig. 1) may involve several configurations of active oxygen atoms around Mn, V, and Mo adsorption sites. The question as to which of them plays the most important role in the catalytic process may be solved experimentally by changing the chemical composition in the brannerite type matrix (cf. (*1, 29, 36*)).

The first step of oxidation of propylene, i.e., abstraction of α-hydrogen (as well as other steps consisting in hydrogen abstraction), is not discussed in detail in this paper. It has been pointed out in the literature that the lateral double bonded oxygens (very short V–O or Mo–O bond) are involved in this process. This idea is taken up in another paper (*37*) where further examples of application of the presently proposed model of active sites are provided. In this context it seems worth noting that in the brannerite-type structure O_G and O_M oxygens may play this role on (201) and (20$\bar{2}$) planes, respectively. It is true that O_M is described as bridging oxygen, but one of its bonds is so long and so weak that the structure may just as well be described as containing fivefold coordinated vanadium.

The method applied in this paper to determine the structure of the active centers should have general significance and be capable of application to other oxide catalysts.

REFERENCES

1. Ziółkowski, J., and Janas, J., *J. Catal.* **81,** 298 (1983).
2. Orgel, L. E., "An Introduction to Transition Metal Chemistry. Ligand Field Theory." Methuen, London, 1960.
3. Germain, J. E., *Intra-Sci. Chem. Rep.* **6,** 101 (1972) and the papers cited therein.
4. Dadyburjor, D. B., Jewur, S. S., and Ruckenstein, E., *Catal. Rev. Sci. Eng.* **19,** 293 (1979), and the papers cited therein.
5. Haber, J., Sochacka, M., Grzybowska, B., and Gołębiewski, A., *J. Mol. Catal.* **1,** 35 (1975).
6. Haber, J., and Witko, M., *J. Mol. Catal.* **9,** 399 (1980).
7. Haber, J., and Witko, M., *Accounts Chem. Res.* **14,** 1 (1981).
8. Adams, C. R., and Jennings, T. J., *J. Catal.* **2,** 63 (1963); **3,** 549 (1963).
9. Voge, H. H., Wagner, C. D., and Stevenson, D. P., *J. Catal.* **2,** 58 (1963).
10. Sachtler, W. M. H., *Rec. Trav. Chim. Pays-Bas* **82,** 243 (1962).
11. Grzybowska, B., Haber, J., and Janas, J., *J. Catal.* **49,** 150 (1977).
12. Sachtler, W. M. H., and de Boer, N. H., Proc. Int. Congr. Catalysis, 3rd (Amsterdam 1964), p. 252, North Holland, Amsterdam, 1965.

13. Boreskov, G. K., *Adv. Catal.* **15,** 285 (1964).
14. Boreskov, G. K., Popovskii, V. V., and Sazonov, V. A., Proc. Int. Congr. Catalysis, 4th (Moscow 1968), Vol. I, p. 439. Akadémiai Kiadó, Budapest, 1971.
15. Winter, E. R. S., *J. Chem. Soc.* 2889 (1968).
16. Moro-oka, Y., and Ozaki, A., *J. Catal.* **5,** 116 (1966).
17. Roiter, V. A., Golodets, G. I., and Pyatnitzkii, Yu. I., Proc. Int. Congr. Catalysis, 4th (Moscow 1968), Vol. I, p. 466. Akadémiai Kiadó, Budapest, 1971.
18. Zhdan, P. A., Shepelin, A. P., Osipova, Z. G., and Sokolovskii, V. D., *J. Catal.* **58,** 8 (1979).
19. Trifirò, F., and Pasquon, I., *J. Catal.* **14,** 412 (1968).
20. Trifirò, F., Centola, P., Pasquon, I., and Jírů, P., Proc. Int. Congr. Catalysis, 4th (Moscow 1968), Vol. I, p. 252. Akadémiai Kiadó, Budapest, 1971.
21. Mitchell, P. C. H., and Trifirò, F., *J. Chem. Soc. A* 3183 (1970).
22. Mars, P., and Maessens, J. G. H., Proc. Int. Congr. Catalysis, 3rd (Amsterdam 1964), p. 266. North Holland, Amsterdam, 1965.
23. Weiss, F., Marion, J., Metzger, J., and Coghon, J.-M., *Kinet. Katal.* **14,** 45 (1973).
24. Ruh, R., and Wadsley, A. D., *Acta Crystallogr.* **21,** 294 (1966).
25. Ng, H. N., and Calvo, C., *Canad. J. Chem.* **50,** 3619 (1972).
26. Calvo, C., and Manolescu, D., *Acta Crystallogr. B* **29,** 1743 (1973).
27. Angenault, J., *Rev. Chim. Miner.* **7,** 651 (1970).
28. Darriet, B., and Galy, J., *Bull. Soc. Fr. Mineral. Crystallogr.* **91,** 325 (1968).
29. Kozłowski, R., Ziółkowski, J., Mocała, K., and Haber, J., *J. Solid State Chem.* **35,** 1 (1980); erratum **38,** 138 (1981).
30. Shannon, R. D., and Prewitt, C. T., *Acta Crystallogr. B* **25,** 925 (1969).
31. Pauling, L., *J. Amer. Chem. Soc.* **51,** 1010 (1929).
32. Baur, W. H., *Naturwissenschaften* **48,** 549 (1961).
33. Ferratis, G., and Catti, M., *Acta Crystallogr. B* **29,** 2006 (1973).
34. Brown, I. D., and Shannon, R. D., *Acta Crystallogr. A* **29,** 266 (1973).
35. Brown, I. D., and Wu, K. K., *Acta Crystallogr. B* **32,** 1957 (1976).
36. Ziółkowski, J., Krupa, K., and Mocała, K., *J. Solid State Chem.*, in press.
37. Ziólkowski, J., *J. Catal.*, **80,** 263 (1983).